Princeton Plasma Physics Laboratory

PPPL- 4320

PPPL- 4320

Electrostatic Dust Detector with Improved Sensitivity

D.P. Boyle, C.H. Skinner, and A.L. Roquemore

June 2008

Prepared for the U.S. Department of Energy under Contract DE-AC02-76CH03073.

18th Int. Conference on Plasma Surface Interactions in Controlled Fusion Devices,
May 26-30, 2008 Toledo, Spain.

Paper no. P1-42

Electrostatic dust detector with improved sensitivity

D. P. Boyle[a], **C. H. Skinner**[b*], and A. L. Roquemore[b].

[a] *Columbia University, New York, NY 10027*

[b] *Princeton Plasma Physics Laboratory, Princeton, NJ 08543, USA.*

Abstract:

Methods to measure the inventory of dust particles and to remove dust if it approaches safety limits will be required in next-step tokamaks such as ITER. An electrostatic dust detector, based on a fine grid of interlocking circuit traces, biased to 30 or 50 V, has been developed for the detection of dust on remote surfaces in air and vacuum environments. Gaining operational experience of dust detection on surfaces in tokamaks is important, however the level of dust generated in contemporary short-pulse tokamaks is comparatively low and high sensitivity is necessary to measure dust on a shot-by-shot basis. We report on modifications in the detection electronics that have increased the sensitivity of the electrostatic dust detector by a factor of up to 120, - a level suitable for measurements on contemporary tokamaks.

PSI keywords: Dust, Erosion & Deposition, ITER.

JNM keywords: P0500 Plasma-Materials Interaction, S0100 Safety of Nuclear Reactors and Components, C0100 Carbon.

PACS codes: 52.40.Hf Plasma-material interactions; boundary layer effects,
52.90.+z Other topics in physics of plasmas and electric discharges.

Corresponding and presenting author address:

Charles H. Skinner, Princeton Plasma Physics Laboratory, POB 451, Princeton NJ 08543 USA.

Email: cskinner@pppl.gov, Phone: 609 243 2214, Fax: 609 243 2665

1. Introduction

The increase in duty cycle and erosion levels in next-step devices will cause a large scale-up in the amount of dust particles produced [1,2,3,4,5]. This has important safety consequences as the dust particles may be radioactive from tritium or activated metals, toxic, and/or chemically reactive with steam or air. A value of 1000 kg of dust inside the ITER vacuum vessel is used for safety assessments; in addition very much smaller quantities on hot surfaces are important in potential chemical reactions. Measuring the dust particle inventory is a challenge in existing tokamaks, let alone one with the radiological environment and scale of ITER. Diagnostics that could provide assurance that ITER is in compliance with its dust inventory limits are in their infancy. A separate challenge is demonstrating techniques that could remove dust from the tokamak, once the limits are approached.

A novel device to detect the settling of dust particles on a remote surface has recently been developed in the laboratory [6,7]. A grid of two closely interlocking conductive traces on a circuit board was biased to 30 – 50 V. Test particles, scraped from a carbon fiber composite tile, were delivered to the grid by a stream of nitrogen. Miniature sparks appeared when the particles landed on the energized grid and created a transient short circuit. Typically, the particles vaporized in a few seconds restoring the previous voltage standoff. The transient current flowing through the short circuit created a voltage pulse that was recorded by standard nuclear counting electronics and the total number of counts was related to the mass of dust impinging on the grid. The device worked well in both at atmosphere and in vacuum environments. The sensitivity has been enhanced by more than an order of magnitude by the use of ultrafine grids [8]. The response to particles of different size categories was compared and the sensitivity, expressed in counts / areal density (mg/cm^2) of particles, was maximal for the finest particles. This is a favorable property for tokamak dust, which is predominantly of micron scale [1]. Larger particles produce a longer current pulse, providing qualitative information on the particle size.

The short circuit is temporary suggesting the device may be useful for the removal of dust from specific areas. The fate of the dust particles has been tracked by measurements of mass gain / loss. Heating by the current pulse caused up to 90% of the particles to be ejected from the grid or vaporized, the removal efficiency depending on the experimental geometry[9], an encouraging result for the management of dust inventories.

Real time measurements of dust on surfaces in contemporary tokamaks are challenging because of the comparatively low dust levels. For example, the average flux of dust in the National Spherical Torus Experiment (NSTX) that accumulated on a glass slide was 5.6 ng/cm^2/discharge, a level below the estimated sensitivity of the 13 x 13 mm grid detector of 36 ng/cm^2/count that was extrapolated from previous measurements at ~ mg/cm^2 dust levels [9]. Experiments with microgram quantities of dust and a large area (51 x 51 mm) grid showed a doubling of sensitivity and linear response down to the lowest measurable masses[10]. The present work is aimed at optimizing the detection electronics to further increase the sensitivity of the detector and enable measurements on contemporary tokamaks. We note that 100 kg of dust evenly distributed on the lower part of ITER amounts to ~ 60 mg/cm^2 so sensitivity will not be an issue for ITER.

2. Experimental setup.

The basic experimental setup has been previously described in ref. [10]. Small (13 x 13 mm) and large (51 x 51 mm) area grids were fabricated by photolithography on Ultralam substrates (in contrast ref. [10] used a laser write process on a PEEK substrate). The traces and intertrace space were 25 μm wide as before and the circuit could standoff at least 60 V. Simulated dust particles were scraped from a CFC tile and pre-filtered through a vibrating mesh with square apertures 104 μm a side. The particles were spread evenly over a dust tray with a 22 mm square double or triple 104 μm mesh bottom; the multiple layers helped retain the dust until needed. The tray was weighed with a Sartorius ME5-F microbalance with 1 μg resolution, 5 g capacity and 50 mm diameter pan that was recalibrated at least twice / day. The dust tray was weighed and moved with an aluminum foil disc underneath to catch any dust that fell through the mesh. Extreme care was used to get high accuracy readings. Small temperature differences between the larger objects and the balance could cause air currents and stabilization times of 5 - 10 minutes. A reading was considered final when it was stable for more than 60 seconds.

The mesh tray was carefully positioned in a holder suspended below a 6” Conflat flange and the flange carefully placed on top of the test chamber (Fig.1). The grid was mounted on the bottom flange and dust was delivered to the grid by mechanically tapping on the chamber. The mass loss of the tray was determined by measuring the mass of tray, foil disk and dust before and after dust delivery. The area on which the dust fell was measured by positioning white paper at the grid position. Most of the dust fell within a 25 x 25 mm square area so that a 51 mm square grid received all of the dust lost by the tray. The fraction of dust falling on the 13 mm square grid was measured with a 13 mm square tray at the grid position and was 28%. The accuracy of the mass measurements was estimated by performing a weighing cycle without tapping the chamber to deliver dust in both air and vacuum conditions. These showed a very small average mass loss of 1.6 ± 1.2 μg that was subtracted from the calculated mass difference delivered to the grid. Extraneous dust was removed from the grid with compressed gas before every trial. For experiments in vacuum, viton gaskets were used to seal the chamber and avoid the mechanical vibration associated with tightening copper gaskets and the chamber was evacuated to 50 - 100 mtorr. A baffle was installed over the evacuation port in the chamber to deflect air currents from the grid during evacuation or venting. To avoid disturbing the dust, pumping was done slowly over 3 - 5 minutes and then the pumping valve closed for dust measurements.

3. Optimization of the Detection electronics.

The short circuit caused by the impinging dust particles caused current to flow in a 51 ohm resistor in the detection circuit. In previous work this signal was conditioned by high and low pass RC filters with a bandpass of 1.3 – 31 kHz (Fig.2). The low pass filter was intended to intended to avoid pulse pile-up and saturation of the electronics for the mg quantities of dust used in earlier experiments. For the present experiment a switch was added that could disable the low pass RC filter to increase the count rate. The signal was then input to an Ortec 550 single channel analyser (SCA) that produced an output pulse every time the input signal decreased past a level of 400 mV and the pulses were counted by an Ortec 775 counter. The input waveforms and output pulses were also recorded by a Tektronix TDS50545B-NV 5 GS/s digital oscilloscope and an example is presented in Fig 3.

With dust delivery to the grid, the voltage across the 51 ohm resistor displayed irregularly shaped pulses of 50 mV to 2 V height with pulse widths of about 1 μs. These typically occurred in bunches of 5 – 10 that continued for several seconds. To assess the relation between SCA threshold and number of output pulses the input waveform with the low pass RC filter disconnected was input to 4 SCAs with settings of 50, 160, 200, 425 mV. Fig. 3 shows that there is a large increase in the number of pulses from the SCA at a setting of 50 mV. There was some pulse pileup at the lower threshold, possibly accentuated by the impulsive nature of the dust delivery by tapping the chamber. Fig. 4 shows the dust detection threshold, expressed as the ratio of the flux of dust falling on the grid to the number of counts generated for 30 and 50 V bias voltages in air and vacuum conditions. The points are an average over 2 or 3 measurements weighted by the uncertainties of the measurements, as there was some variation in sensitivity between trials. However, the relative improvement from reducing the SCA setting from 400 mV to 50 mV was consistent between trials, and reduced the detection threshold by a factor of 4-9x depending on conditions. Compared to the value in air, the detection threshold under vacuum increased by 7-15x at 50 V and 2x at 30 V bias.

The largest number of counts was obtained by disconnecting the low pass RC filter and using a 50 mV SCA threshold. Fig. 5 shows the results in air and vacuum for 13 and 51 mm grids and for comparison previous results from ref. [10] with the low pass RC filter and 400 mV SCA threshold. It can be seen that the sensitivity has increased by 50-120x compared to the earlier results. In these comparisons, the flux of dust on the 13 mm grid is calculated as 28% of the mass loss by the tray (see sect. 2) divided by the area of the 13 mm grid. For the 50 mm grid case the flux is the mass loss divided by the area of the 50 mm grid. In ref. [10] the relative sensitivity of the 51 mm grid on the PEEK substrate was 2x higher than previous measurements with a 13 mm grid on the Ultralam substrate, a factor much lower than the 16x increase in area. In the present work both 13 and 51 mm grids were on Ultralam substrates and a 6x higher number of counts was seen from the larger grid [conditions: 30 V bias voltage, air, 50 mV SCA]. Covering the 51 mm grid with a 13 mm aperture resulted in the same number of counts as the 13 mm grid. The scatter of the data points around the linear fit is attributed to variations in the dust delivery to the grid and in the subsequent pulse pile up. The sublinear increase in the response with grid area could also be due to pulse pileup in the larger grid.

The dependence on number of counts with bias voltage was also investigated. Lower voltages may result in multiple pulses from the same particle if it is not immediately ejected from the grid. The sensitivity of the 13 mm grid increased a factor of two when the bias voltage was decreased from 50 to 25 V while the 51 mm grid did not show a clear dependence of sensitivity on bias voltage [conditions: air, 50 mV SCA]. On the other hand, bias voltages much lower than 30 V could result in a continuous short when exposed to dust particles.

4. Conclusions

The ability to measure ultralow levels of dust is important for demonstrations of time resolved detection of dust on surfaces in contemporary tokamaks. We have optimized the detection electronics for the electrostatic dust detector by removing a low pass RC filter and lowering the SCA setting from 400 mV to 50 mV. This resulted in an increase in sensitivity, by a factor of up to a 120x and corresponding reduction in the detection threshold from 2-5 ng/cm^2/count to 0.02 ng/cm^2/count for a 51mm square grid at 30 V bias voltage. There was not a strong dependence of sensitivity on bias voltage and power supply current limit. The sensitivity is now suitable for contemporary tokamaks. Tests on NSTX are currently in progress and the results will be reported elsewhere.

Acknowledgments

The authors thank T. Holoman, R Marsala and T. Provost for technical assistance. D. Boyle acknowledges support from the 2007 National Undergraduate Fellowships in Plasma Physics and Fusion Energy Sciences. The grids were supplied by MicroConnex of Snoqualmie, WA. This work was funded by U.S. DOE Contract Nos. DE-AC02-76CH0307.

Figure Captions:

Fig. 1 Dust tower used to deposit microgram quantities of dust on electrostatic grid in air or vacuum environments. The dust tray was weighed and loaded in the stand on the left. The flange + tray + catch foil was then transferred to the test vessel on the right.

Fig. 2. Circuit used to convert dust signals to discrete counts.

Fig. 3 Waveform at input to SCAs (a) and corresponding 6V SCA output pulses, offset for clarity, for the 13 mm grid, with bias voltage 30 V in air. Label (b) denotes the 400 mV SCA setting and output pulses and label (c) the 50 mV SCA setting and output pulses.

Fig. 4 Detection threshold as a function of SCA threshold. The points represent a weighted average, the lines are to guide the eye. The labels on the right denote the bias voltage and conditions. The dashed line followed to the left shows a 7x decrease in detection threshold as the SCA setting is decreased from 400 mV to 50 mV. The vertical arrows show a 2x and 10x increase in detection threshold at 30V and 50V respectively in changing from air to vacuum conditions.

Fig. 5 Overall detection threshold for (a) 13 mm grid and (b) 50 mm grid with the low pass RC filter off under air and vacuum conditions. The lines are a linear fit to the data.

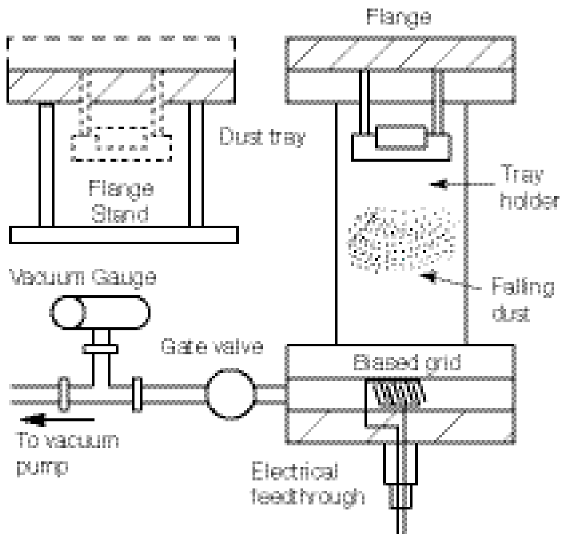

Fig. 1. Dust tower used to deposit microgram quantities of dust on electrostatic grid in air or vacuum environments. The dust tray weighed and loaded in the stand on the left. The flange + tray + catch foil was then transferred to the test vessel on the right.

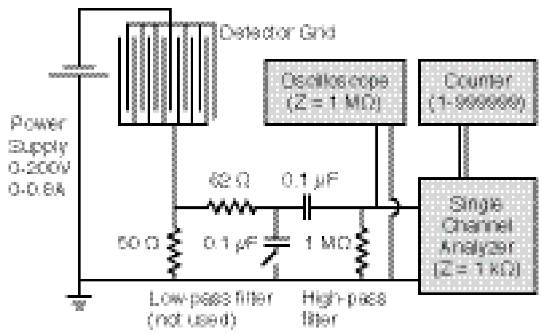

Fig. 2. Circuit used to convert dust signals to discrete counts.

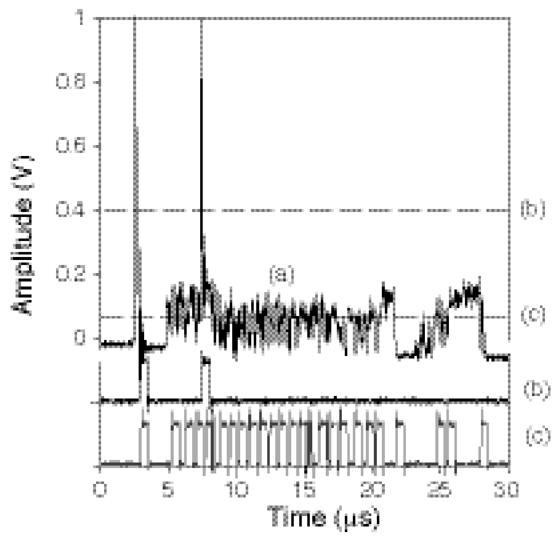

Fig. 3 Waveform at input to SCAs (a) and corresponding 6V SCA output pulses, offset for clarity, for the 13 mm grid, with bias voltage 30 V in air. Label (b) denotes the 400 mV SCA setting and output pulses and label (c) the 50 mV SCA setting and output pulses.

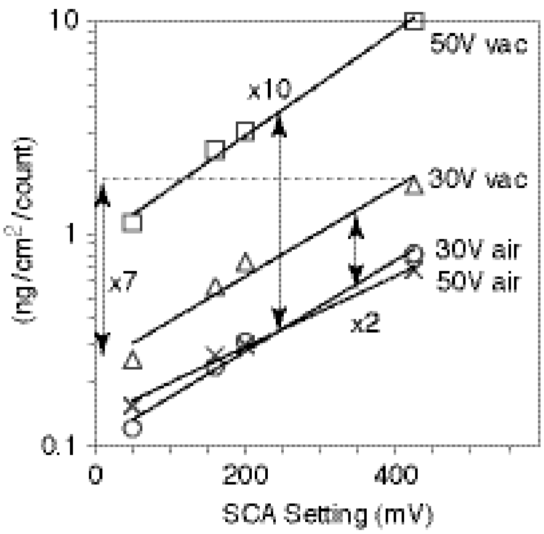

Fig. 4. Detection threshold as a function of SCA threshold. The points represent a weighted average of 2-3 trials, the lines are to guide the eye. The labels on the right denote the bias voltage and conditions. The dashed line followed to the left shows a 7x decrease in detection threshold as the SCA setting is decreased from 400 mV to 50 mV. The vertical arrows show a 2x and 10x increase in detection threshold at 30V and 50V respectively in changing from air to vacuum conditions.

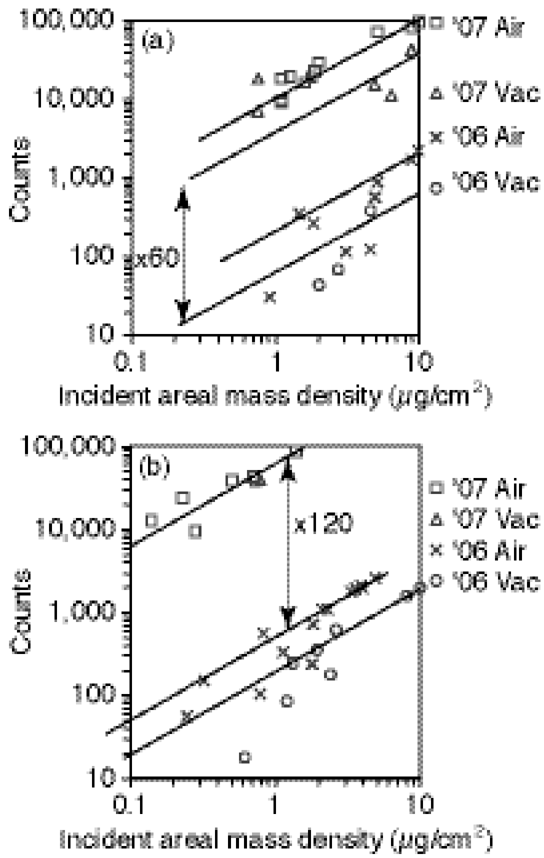

Fig. 5 Overall detection threshold for (a) 13 mm grid and (b) 50 mm grid with the low pass RC filter off under air and vacuum conditions. The lines are a linear fit to the data.

References:

[1] G. Federici, et al., Nucl. Fus. 41 (2001) 1967.

[2] J. P. Sharpe, D. A. Petti, H. –W Bartels, Fus. Eng & Des., 63-64 (2002) 153.

[3] Z. Wang et al., in New Aspects of Plasma Physics, Proceedings of 2007 ICTP Summer College on Plasma Physics, Trieste 30 July - 24 August 2007, ed. P. K. Shukla, L. Stenflo and B. Eliasson, World Scientific (Singapore) 2008.

[4] J. Winter, Plasma Phys. Controlled Fusion 40 (1998) 1201.

[5] M. Rubel *et al.*, Nucl. Fusion 41 (2001) 1087.

[6] A. Bader, C. H. Skinner, A.L. Roquemore, and S. Langish, Rev. Sci. Instrum. 75, (2004) 370.

[7] C. H. Skinner, A. L. Roquemore, A. Bader and W. R. Wampler, Rev. Sci. Instrum., 75 (2004) 4213.

[8] C. Voinier, C. H. Skinner and A. L. Roquemore, J. Nucl. Mater. 346 (2005) 266.

[9] C. V. Parker, C. H. Skinner and A. L. Roquemore, J. Nucl. Mater., 363-365 (2007) 1461.

[10] C. H. Skinner, R. Hensley and A. L. Roquemore, J. Nucl. Mater., 376 (2008) 29–32.

The Princeton Plasma Physics Laboratory is operated
by Princeton University under contract
with the U.S. Department of Energy.

Information Services
Princeton Plasma Physics Laboratory
P.O. Box 451
Princeton, NJ 08543

Phone: 609-243-2750
Fax: 609-243-2751
e-mail: pppl_info@pppl.gov
Internet Address: http://www.pppl.gov